Journal of
Manufacturing and Materials Processing

MDPI

Article

Comparison of 2D and 3D Surface Roughness Parameters of AlMgSi0.5 Aluminium Alloy Surfaces Machined by Abrasive Waterjet

Csaba Felhő *, Krisztina Kun-Bodnár and Zsolt Maros

Institute of Manufacturing Science, University of Miskolc, H-3515 Miskolc, Hungary; krisztina.bodnar@uni-miskolc.hu (K.K.-B.); zsolt.maros@uni-miskolc.hu (Z.M.)
* Correspondence: csaba.felho@uni-miskolc.hu

Abstract: The use of 3D roughness parameters is increasingly gaining ground in various areas of engineering, especially in academic research. In many cases, however, these studies primarily cover the illustration of the character of the surfaces, the interpretation of areal numerical roughness values is often disputed. The goal of this paper is to examine how the 2D and 3D roughness parameters change in the case of anisotropic surfaces, such as surfaces cut with an abrasive water jet. For this purpose, abrasive water jet cutting experiments were performed on AlMgSi0.5 aluminum alloy using different technological parameters. After the experiments, two amplitude-type 3D roughness parameters (S_a and S_z) of the cut surface and four profile parameters (R_a, R_z for roughness and P_a, P_z for raw profile) were measured at five different depths. Our conducted research indicates that the 3D parameters represent a kind of average value for certain roughness characteristics and a maximum value for others. The paper also reports on how these roughness characteristics change as a function of feed speed.

Keywords: surface roughness; comparison of 2D and 3D roughness; abrasive waterjet cutting

check for updates

Academic Editor: Steven Y. Liang

Received: 30 January 2025
Revised: 21 February 2025
Accepted: 26 February 2025
Published: 2 March 2025

Citation: Felhő, C.; Kun-Bodnár, K.; Maros, Z. Comparison of 2D and 3D Surface Roughness Parameters of AlMgSi0.5 Aluminium Alloy Surfaces Machined by Abrasive Waterjet. *J. Manuf. Mater. Process.* **2025**, *9*, 80. https://doi.org/10.3390/jmmp9030080

Copyright: © 2025 by the authors. Licensee MDPI, Basel, Switzerland. This article is an open access article distributed under the terms and conditions of the Creative Commons Attribution (CC BY) license (https://creativecommons.org/licenses/by/4.0/).

1. Introduction

Abrasive waterjet (AWJ) cutting is a reliable technology for cutting difficult-to-machine materials, which may have several benefits over traditional cutting processes. One of the biggest superiority of the process is that a wide variety of materials can be processed with it (hard materials, metals, non-metals, composites, ceramics, etc.) [1].

AWJ can be used to cut most materials from macro to micro scales [2]. It has additional features that can be favored over other processes: it does not generate heat at the cutting zone [3]; thus, the material integrity of the cut surface is left intact [4]; faster material removal rate compared to the wire EDM process [5], capable of cutting thick parts up to 250 mm [6]; no thermal distortion affecting the work materials yet able to cut complex shapes; minimal cutting force applied to the work materials, resulting in improved dimensional accuracy with negligible deformation [7].

However, despite that the surface roughness may be considered better than some other cutting methods, e.g., CO_2 laser beam cutting [8], one of the disadvantages of the process is that the roughness of the cut surface is not homogeneous, due to the continuous decrease in the energy of the jet as it penetrates into the material; the surface microgeometry also changes, with striation marks, distorted kerf geometry, and delamination potentially occurring, which can cause changed surface microtopography [9]. Additionally, the AWJ process is applicable not just for cutting different materials, but also for "milling" flat

surfaces, as demonstrated in [10], where an experimental model was developed that connected the overall cavity depth with the depth and width of an individual slot and the lateral feed.

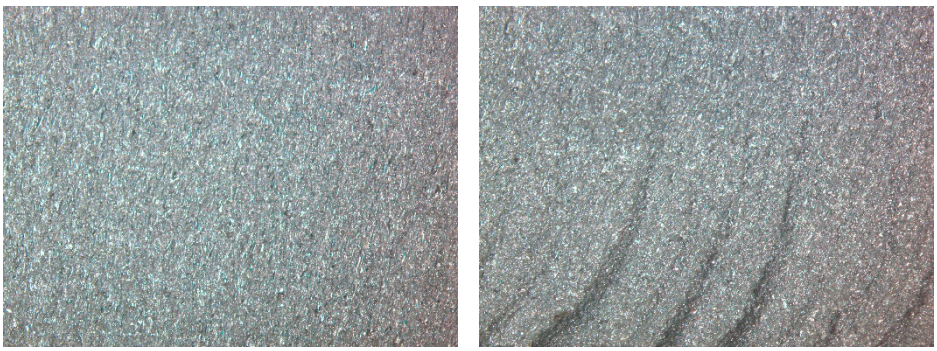
As a result, the numerical characterization of the roughness of the cut surface with traditional two-dimensional roughness parameters [11] encounters obstacles, and the values are also highly dependent on the thickness of the material [12]. It was also revealed that abrasive flow rate and standoff distance have also a great effect on the quality of the cut surface [13]. Magsipoc et al. [14] also came to the conclusion based on their tests that the three-dimensional roughness parameters provide a much more representative analysis of the surface structure, and eliminate the bias that can occur by using 2D measurements (e.g., loss of significant details, relationship of features perpendicular to shear directions, etc.). Despite this, some researchers still believe, that for more traditional manufacturing processes, two-dimensional roughness values may also be suitable, as it was shown for honing [15], tangential turning [16], milling [17,18] and drilling [19]. However, other researchers have found that it is more appropriate to use three-dimensional roughness parameters even for surfaces machined with traditional methods [20,21]. In tribology, extreme values matter for both dry and lubricated contacts. Therefore, [22] emphasizes that a 3D analysis is more suitable for assessing surface quality and better represents the topography's characteristics.

Furthermore, researchers have made many attempts to try to find correlations between 2D and 3D roughness parameters [23,24]. However, it should also be noted here, that these correlations can only be considered good for a given type of surface, as some others may exhibit totally different properties [25]; therefore, the roughness parameter to be used should be selected according to the machining process [26]. Rosentritt et al. [27] found that the values of the 2D and 3D roughness parameters also depend on the measuring principle of the instrument used (contact profilometry (CP), confocal 3D laser scanning microscope (CLSM), and scanning electron microscope (SEM) were tested in the paper). They have found that the measured values with CLSM are higher than the values with CP. Three-dimensional parameters are now spreading because of the use of the Alicona (Alicona Gmbh, Grambach, Austria), Leica (Leica Camera AG, Wetzlar, Germany), Sensofar (Sensofar Metrology, Terrassa, Spain), etc. roughness meter and profile meters. The initial works with touch probes make longer inspection times, but even with that people used them as was shown in [28] for molds. It should also be considered, that a single 3D surface measurement typically does not provide enough data for statistical surface quantification, although fewer measurements are generally needed compared to 2D methods [29]. Additionally, the surface roughness parameters can be used for many other purposes in addition to the characterization of the surface quality of the components, an example of its use in tribology is shown in [30].

The present research investigated how two- and three-dimensional surface roughness parameters relate to each other in the case of surfaces cut with an abrasive water jet. In industrial practice, two-dimensional profile roughness parameters are most often used to classify machined surfaces. However, these do not always provide a complete picture of the nature of the machined surface.

In this research, the results of studies on the differences and comparisons of these parameters in surfaces machined with the abrasive waterjet process are presented. The topography of surfaces cut with an abrasive water jet can vary greatly depending on the cut sheet thickness and the technological data used, even with identical material qualities, nozzle geometries, or machine equipment; therefore, the tests were carried out under different process parameters.

Figure 1 shows the cut surface of a 10 mm thick AlMgSi0.5 aluminum alloy at two different feed speeds. This figure clearly illustrates that there is a significant difference in the topography (roughness) of the two surfaces, although their machining only differs in the feed speed of the cutting head. In Figure 1a, at low feed speed, the surface is fine, smooth, and even, so it can be considered practically isotropic. In Figure 1b at high feed speed, the surface is rougher than the previous one, uneven, and can be vertically divided into three characteristic zones (smooth, transitional, and striation zones).



(**a**) (**b**)

Figure 1. Surface of AlMgSi0.5 alloy cut with abrasive water jet at feed speeds of (**a**) v_f = 50 mm/min and (**b**) v_f = 350 mm/min.

It can also be observed from the figure that the surface roughness is generally much smaller on the entering side of the jet (top) than on the exiting side (bottom). This phenomenon is a characteristic of all jet machining processes and can be explained primarily by the loss of energy of the jet and by the fact that the workpiece is not yet cut in its full cross-section when the cutting head advances. This then results in the formation of characteristic, so-called striations (deflection lines) on the surface. The magnitude of this phenomenon depends on the applied technological parameters, and in the case of a given material and sheet thickness, primarily on the magnitude of the energy input [31]. The technological parameters affect not only the surface roughness, but also the shape and depth of kerfs [32].

Based on the above, abrasive waterjet cutting usually results in a clearly anisotropic surface topography, where the surface roughness can vary significantly between the entry and exit sides. In the case of surfaces with anisotropic roughness, it may be interesting to see how much the areal (3D) roughness parameters characterize the surface and how they relate to the two-dimensional, profile-wise roughness parameters measured at different locations (depths). A series of experiments were conducted on a 10 mm thick AlMGSi0.5 aluminum alloy to investigate this issue.

2. Materials and Methods

The material used for the experiments was AlMgSi0.5 (EN AW-6060, DIN 3.3206) aluminum alloy. The AlMgSi0.5 (EN AW 6060) aluminum alloy is a versatile and commonly used alloy due to its good mechanical properties and corrosion resistance. It is a heat-treatable alloy with excellent corrosion resistance, weldability, and good machinability [33]. The chemical composition of the alloy is summarized in Table 1.

Table 1. Chemical composition of AlMgSi0.5 aluminum alloy.

Material	Si (%)	Mg (%)	Fe (%)	Cr (%)	Cu (%)	Mn (%)	Ti (%)	Zn (%)
AlMgSi0.5	0.3–0.6	0.35–0.6	0.1–0.3	<0.05	<0.1	<0.1	<0.1	<0.15

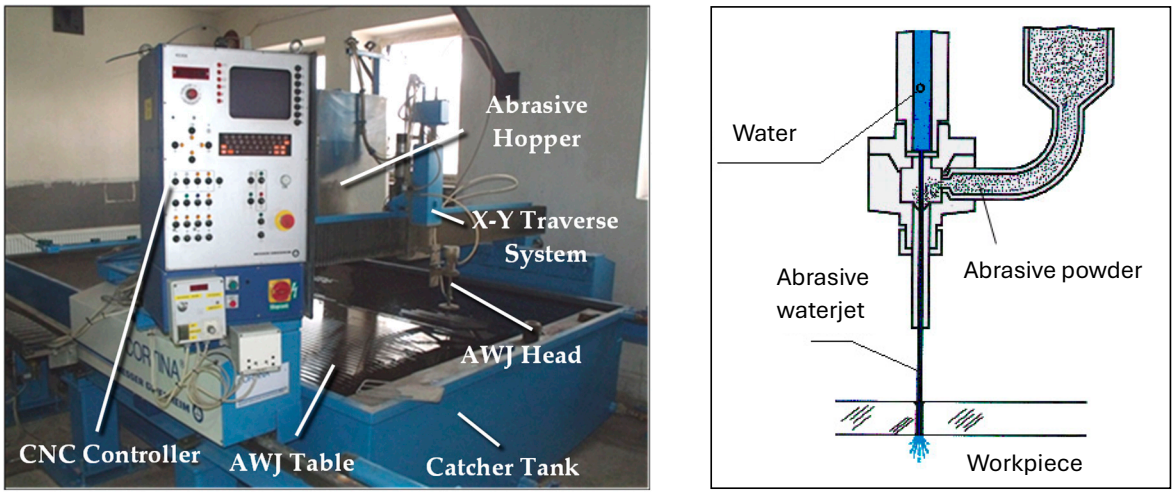
AlMgSi0.5 contains magnesium (Mg) and silicon (Si) as its main alloying elements, with 0.5% silicon content. This gives the alloy its strength and excellent response to heat treatment. The machinability of AlMgSi0.5 is generally good. The presence of silicon improves its ability to be machined, as it creates a fine, smooth surface finish. However, due to the alloy's relatively high strength, special attention is needed when machining to avoid tool wear [34].

The characteristic mechanical properties of the material are summarized in Table 2. During the experiments, cuts were made on a 10 mm thick sheet with different technological parameters.

Table 2. Mechanical properties of AlMgSi0.5 aluminum alloy.

Conventional yield strength $R_{p0.2}$ (MPa)	65–160
Tensile strength, R_m (MPa)	130–215
Specific elongation at break, A (%)	8–16
Hardness (HB)	45–65
Young-modulus (GPa)	69
Fracture toughness ($MPam^{1/2}$)	34

The investigations were performed on an INNO PUMP 36HD type abrasive waterjet cutting machine (INNOWELD-Metallverarbeitung GmbH, Mürzzuschlag, Austria) (Figure 2a). The essence of abrasive water jet cutting is that a small diameter, high-speed jet of water-abrasive powder mixture is directed onto the surface to be machined, which separates the material from the workpiece due to the high energy density (Figure 2b). Due to the feeding movement of the cutting head, arbitrary contours can be cut.



(**a**) (**b**)

Figure 2. The AWJ system overview: (**a**) the INNO PUMP 36HD type abrasive waterjet cutting machine; (**b**) schematic diagram of the process.

The abrasive powder used was Barton Garnet #80. Variables were the water pressure, the abrasive flow rate, and primarily the feed speed of the cutting head. The specific data are shown in Table 3. When choosing the values of feed speeds, it was considered that increasing the cutting speed results in some deterioration of the surface roughness, while the material removal efficiency improves. Based on previous experiments [35,36], the application of the investigated range (50–300 mm/min) seems reasonable.

Table 3. Characteristics and parameters of the cutting experiments.

Characteristic	Cut Through Test
Type of machine tool	INNO PUMP-36HD
Workpiece material	AlMgSi0.5 Al-alloy
Thickness of the material [mm]	10
Diameter of water nozzle [mm]	0.25
Diameter of abrasive nozzle [mm]	0.8
Stand of distance [mm]	2
Abrasive mass flow rate [g/min]	7
Water pressure [bar]	3500
Feed speed [mm/min]	50, 100, 150, 200, 250, 300

After the machining, the surface roughness was measured in the laboratory of the Institute of Manufacturing Science of the University of Miskolc using the AltiSurf 520 three-dimensional surface topography tester device (Altimet SAS, Marin, France) (Figure 3). The applied sensor was the CL4 confocal chromatic probe with an MG35 magnifier, and the measurement speed was 1000 µm/s. During the evaluation, profile and areal roughness characteristics were also determined to characterize the roughness of the surfaces. Figure 4 shows a view of the areal roughness measurement. The test pieces are the same as those in Figure 1.

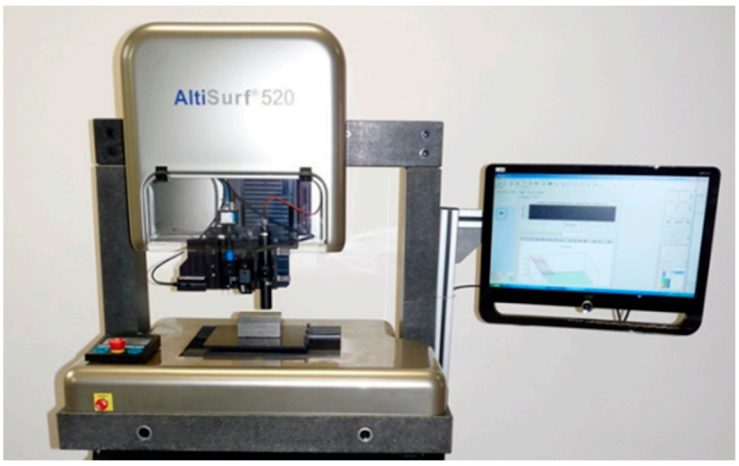
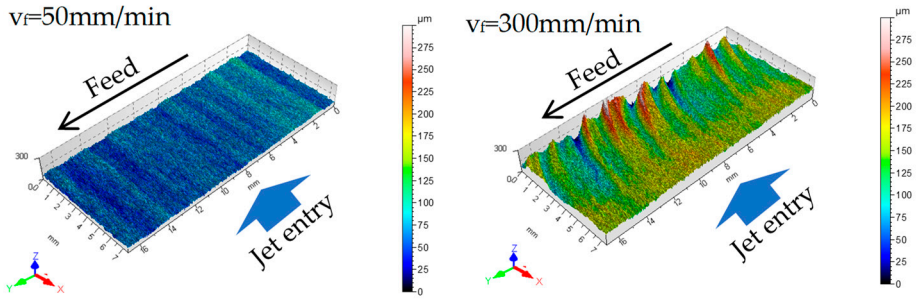


Figure 3. AltiSurf 520 three-dimensional surface topography device.



(**a**) (**b**)

Figure 4. Areal roughness images of the cut surface of AlMgSi0.5 alloy cut with abrasive water jet when using feed speeds (**a**) v_f = 50 mm/min; and (**b**) v_f = 350 mm/min.

Here, the significant difference between the roughness of the two surfaces is even more striking. The areal roughness parameters S_a, S_t were evaluated.

The 2D parameters were measured at 5 different depths from the jet entry side (0.15 mm, 0.2 mm, 3.75 mm, 5.5 mm, 7.5 mm, see Figure 4) along the profile. Since

there were no filters when measuring the areal parameters, we also chose features for the 2D parameters that are unfiltered; i.e., we determined the raw profile indexes P_a and P_t.

3. Results and Discussion

Figure 5 shows the variation in the three-dimensional roughness parameter S_z and the corresponding two-dimensional roughness parameter P_z as a function of the layer depth. Since S_z was measured on the entire (7.5 × 16.5 mm^2) surface, it characterizes the whole surface; therefore, S_z is constant with respect to the surface; i.e., it can be represented as a horizontal line as a function of the depth.

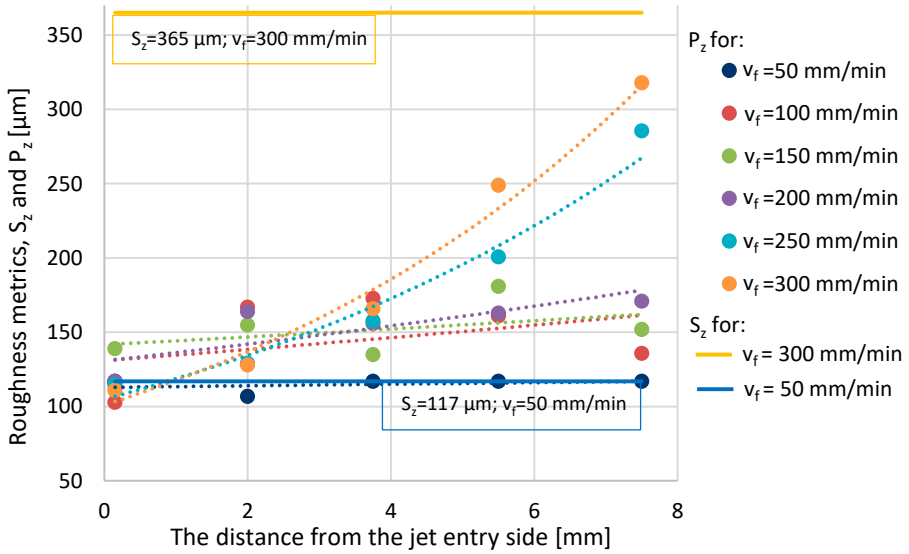


Figure 5. Variation in the roughness parameters S_z and P_z as a function of the distance from the jet entry side.

Based on Figure 5, it can be stated that the total profile error P_t increases as a function of depth. The lower the feed speed, the smaller the total profile error at the exit side. On the entry side—where the energy of the jet is still very high—the change is not so clear and the roughness of the surfaces has relatively small deviations from each other at different feeds. The P_z values are smaller than the measured S_z value, which follows from the fact that the P_z and S_z values are a kind of "maxima", so the S_z data characterizing the entire area are obviously more than that measured along each profile. At the same time, the P_z maximum measured at a feed speed of v_f = 300 mm/min is already very close to the S_z value characterizing the area, because on the exit side, at high feeds, the highest roughness values were obtained. It is also interesting to observe that at low feed speeds (v_f = 50 mm/min), where the roughness of the machined surface is nearly isotropic, the P_z value is essentially constant and almost identical to the S_z value as a function of the layer depth.

Figure 6 shows the variation in the three-dimensional roughness parameter S_a and the two-dimensional roughness parameter P_a as a function of layer depth.

Based on Figure 6, it can be stated that the average profile error P_a increases as a function of depth. Similarly in the case of the P_z values, here too the lower the feed speed, the smaller the average profile error and the average areal roughness S_a. This is primarily noticeable at the exit side.

On the entry side, the profile errors are also almost identical along the depth. Since the average areal roughness S_a gives an average value of the entire measured surface, its value is greater at the entry side and smaller at the exit side than the P_a values measured along the profile. It is almost identical to the value obtained on the profile measured in the middle.

Compared to Figure 5, it can be observed that in this case the measured values of S_z/S_a and the ratio of P_z/P_a are both approximately 10–12. In traditional chip removal processes, this ratio is usually estimated at a value of around 5. At low feed speeds (v_f = 50 mm/min), there is no change in the depth function here either, which also indicates that the surface topography is isotropic.

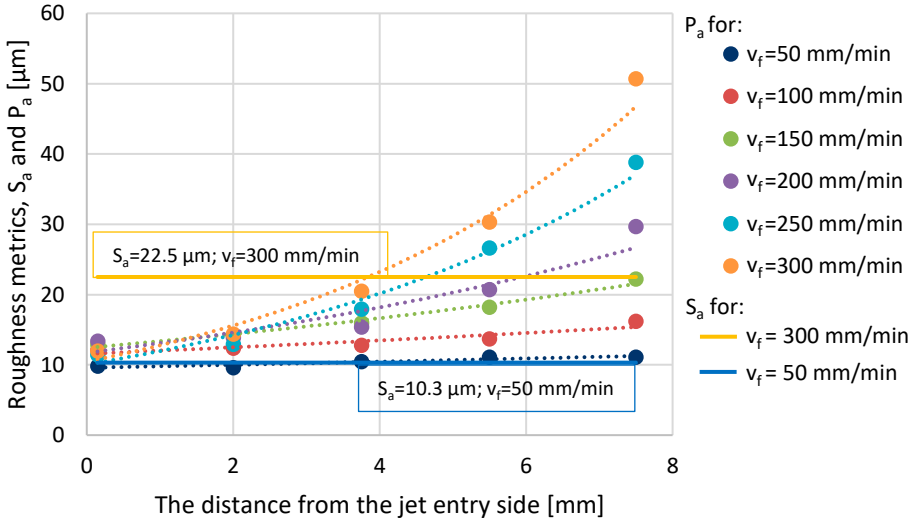


Figure 6. Variation in roughness metrics S_a and P_a as a function of distance from the jet entry side.

Figure 7 shows the variation in the roughness parameters R_a and S_a as a function of depth. Researchers often use these two parameters to characterize the roughness of surfaces and compare them, although as previously shown, there is a significant difference between them, so a numerical comparison of their values is not always useful.

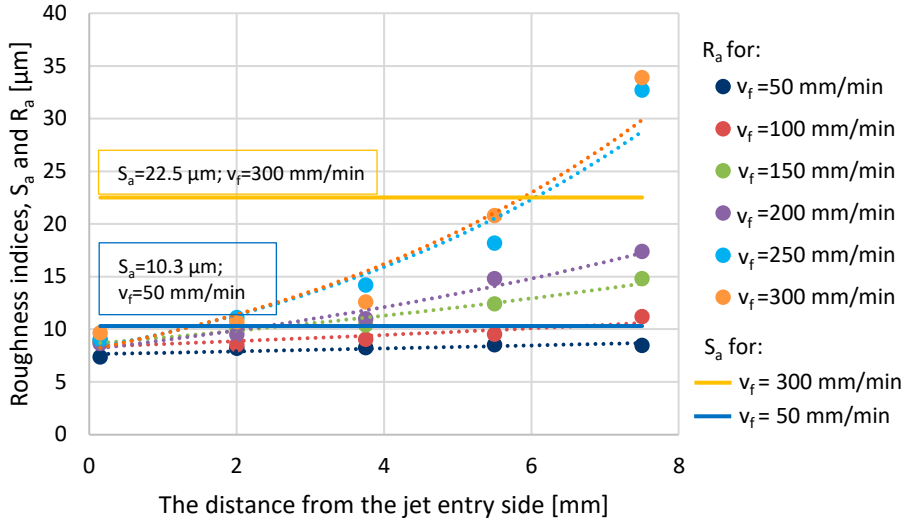


Figure 7. Variation in roughness indices S_a and R_a as a function of distance from the jet entry side.

It should be noted that Figure 7 is almost identical in its main character to Figure 6. This follows from the fact that the R_a and P_a metrics are similarly defined values; the only difference is that R_a represents filtered (roughness) and P_a shows unfiltered (raw) values. Therefore, the R_a values themselves are smaller than the P_a values of the same measured profile. In Figure 7, it can be observed again that, at small feeds, the surface roughness hardly changes as a function of depth; the surface roughness itself can be considered isotropic.

Figure 8 shows the surface topography as a function of feed speed. It is clear from the figure that the surface roughness clearly increases as a function of feed speed.

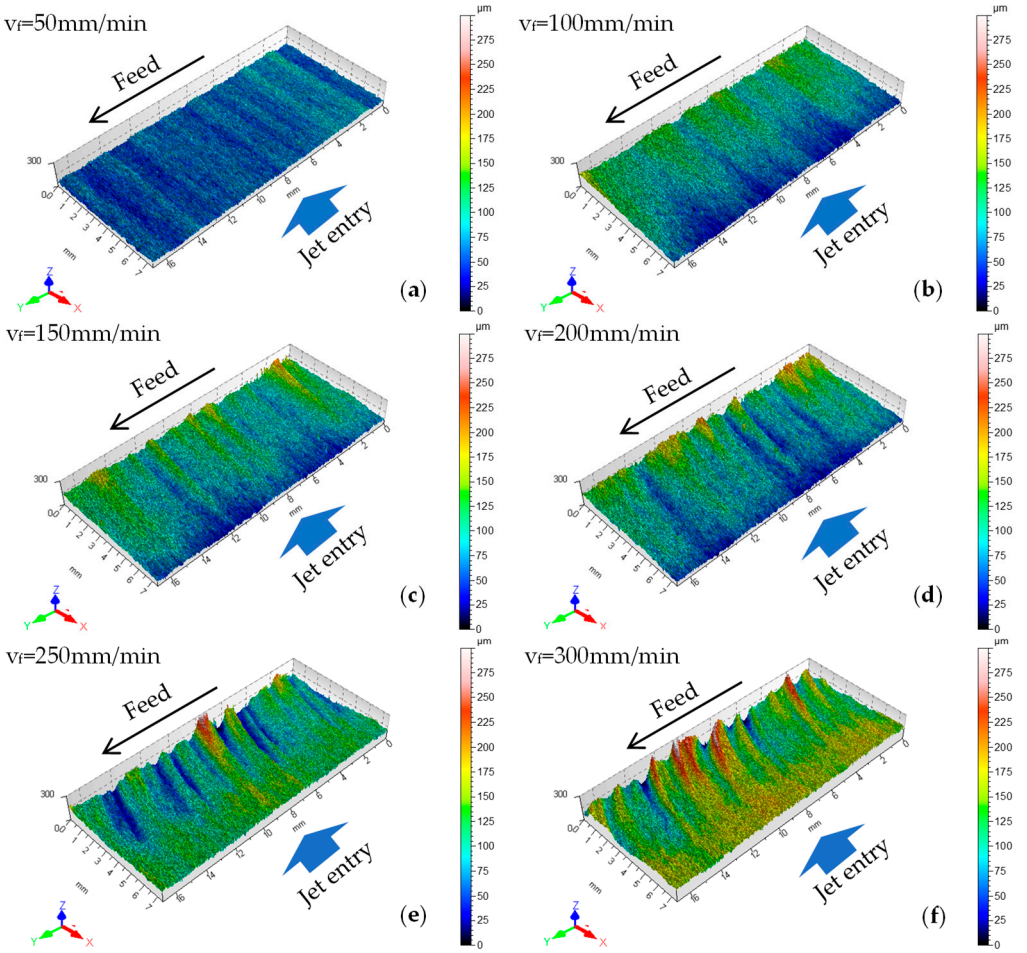


Figure 8. Surface topography of the cut surfaces for different feed speeds: (**a**) v_f = 50 mm/min; (**b**) v_f = 100 mm/min; (**c**) v_f = 150 mm/min; (**d**) v_f = 200 mm/min; (**e**) v_f = 250 mm/min; (**f**) v_f = 300 mm/min.

Figure 9 illustrates the variation in the areal average S_a and maximum S_z roughness as a function of the cutting head feed speed.

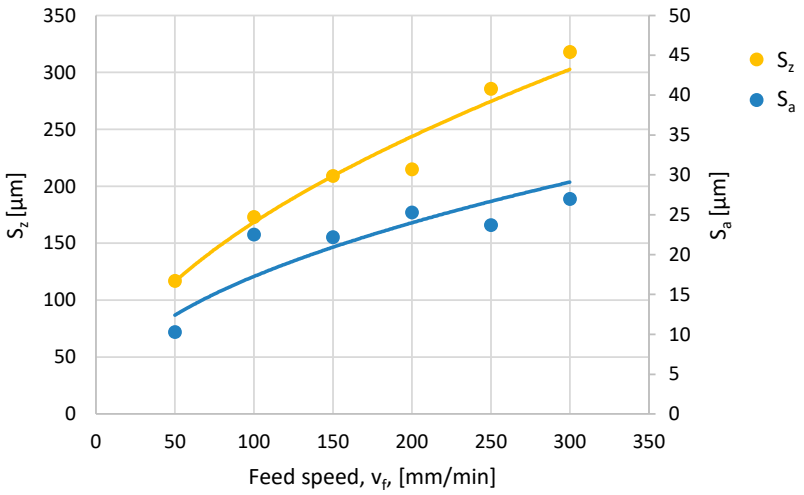


Figure 9. Variation in roughness indices S_a and S_z as a function of feed speed.

It is clearly visible from Figure 9 that the S_z values increase as a function of the feed speed. This finding can also be established by visual inspection of the cut surfaces (Figure 1). At the same time, the increase in the S_a values is slight; after a large jump following the lowest feed speed value, it only increases slightly. It can also be established from the figure that the S_z/S_a value ratio shows a value of approx. 10–12 times.

Figure 10 shows the variation in the P_z roughness as a function of the feed speed, along profiles measured at different depths.

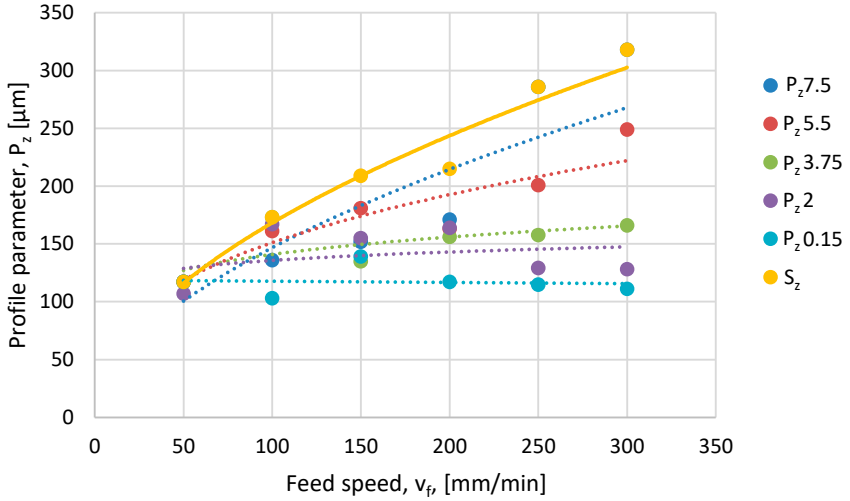


Figure 10. Variation in profile parameter P_z as a function of feed speed at different depths.

Based on Figure 10, it can be stated that the P_z profile parameter basically increases by increasing the feed speed. This is especially noticeable near the exit side. On the entry side, the P_z value does not typically depend on the feed speed, its value can be considered to be approximately constant. The further we move away from the entry side, i.e., the weaker the energy of the jet, the more noticeable the increase in P_z is. We have also plotted the areal roughness values of S_z in Figure 10. It is clear that this is a kind of upper-bound envelope for the different P_z values.

Figure 11 shows the average profile error P_a as a function of feed speed, for profiles measured at different depths.

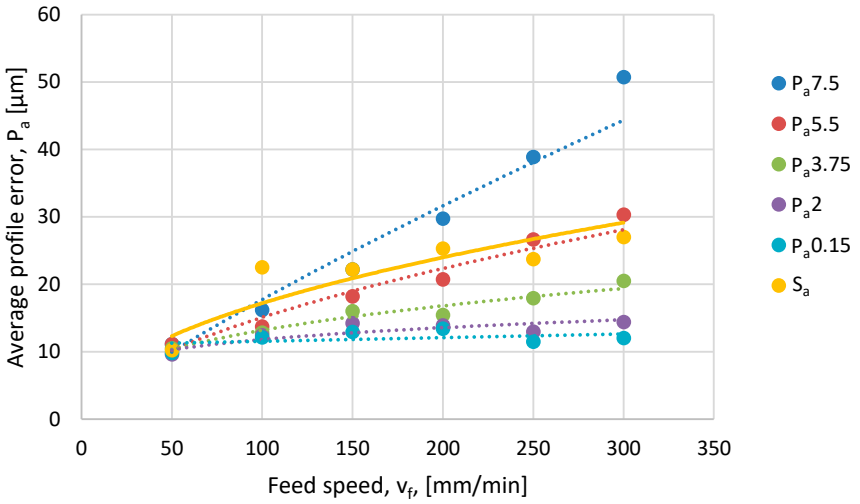


Figure 11. Variation in average profile error P_a as a function of feed speed at different depths.

The profile error P_a, similarly to P_z, increases with increasing feed speed, which is not clear near the entry side, where the magnitude of P_a is essentially independent of the magnitude of the feed speed. Figure 11 also shows the average areal roughness S_a, which is located in the middle of the depicted curve set, as it is a kind of average of the entire area, both at the entry and exit sides.

4. Conclusions

Based on the cutting experiments and the carried-out evaluation of data, the following conclusions were made:

- The topography of surfaces cut with an abrasive water jet is usually highly direction-dependent, i.e., anisotropic. Creating surfaces with nearly isotropic roughness is only possible when applying a very high energy input (e.g., low feed speed);
- The roughness parameters measured along the profile (P_a, P_z) do not match the corresponding areal roughness parameters S_a, S_z in terms of their numerical values in the case of surfaces cut with an abrasive water jet. A match is generally not expected, because areal parameters always give an image of a smaller or larger area, while 2D parameters give an image of a single profile. This is especially true in the case of surfaces with anisotropic roughness;
- This led to the observation that in the case of maximum-type parameters (P_z, S_z), the areal ones are always larger. The relationship between the average parameters (e.g., P_a, S_a) depends on where the 2D roughness profile is taken. In the case of a surface machined with an abrasive water jet, the Pa values are lower on the entry side and the Sa values are lower on the exit side;
- The P_z/P_a and S_z/S_a ratios for the roughness of surfaces machined with an abrasive water jet were measured to be approximately 10–12;
- The P_a, P_z, S_a, and S_z values basically increase as a function of the distance from the entry side. At low feed speeds, this increase is not significant, but can be strongly observed when using higher feed speeds;
- As the feed speed increases, we also experience an increase in the roughness parameters, which is not typical near the entry side; here, the roughness hardly changes because the jet has sufficiently high energy, which is sufficient for adequate material removal even at low feed speeds;
- The R_a average roughness value, widely used in industry, behaves analogously to the P_a value; its value is much smaller than that, so it is even less comparable with the S_a values measured in the field.

As a general summary, it can be stated that for surfaces cut with an abrasive water jet, the numerical values of the areal (S_a and S_z) and two-dimensional (P_a, P_z) roughness measured along the line are not the same. The S_z values are always larger than the P_a values, and the S_a values are a kind of average of the P_a values measured at different depths. If we want to make a comparison between the areal and profile roughness, we should not compare the S_a and R_a values, but the S_a-P_a and S_z-P_z measurements. This does not mean significant additional time for two-dimensional roughness measurements traditionally used in industrial practice; it merely requires proper adjustment of the roughness measuring instrument. One of the goals of our further research work is to determine in which parts and over what areas the areal roughness parameters need to be measured in order to characterize the surfaces cut with an anisotropic abrasive water jet.

Author Contributions: Conceptualization, Z.M. and K.K.-B.; methodology, Z.M.; software, C.F.; validation, Z.M. and C.F.; formal analysis, C.F.; investigation, K.K.-B.; resources, C.F.; data curation, Z.M.; writing—original draft preparation, Z.M. and K.K.-B.; writing—review and editing, C.F.;

visualization, K.K.-B.; supervision, Z.M.; project administration, C.F.; funding acquisition, C.F. All authors have read and agreed to the published version of the manuscript.

Funding: This research received no external funding.

Data Availability Statement: The original contributions presented in this study are included in the article material. Further inquiries can be directed to the corresponding author.

Acknowledgments: Sincere thanks to the University of Miskolc, Hungary, Faculty of Mechanical Engineering and Informatics, Institute of Manufacturing Science, and Institute of Materials Science and Technology, for providing academic support and to DINAS Ltd., Miskolc, Hungary, for providing the necessary resources and technical assistance that contributed significantly to this research.

Conflicts of Interest: The authors declare no conflicts of interest.

References

1. Kroupa, T.; Dana, M.; Zetek, M. Abrasive Waterjet Cutting. In Proceedings of the 28th DAAAM International Symposium, Zadar, Croatia, 8–11 November 2017; DAAAM International: Vienna, Austria, 2017; Volume 1, pp. 0493–0499.
2. Liu, H.-T. "7M"Advantage of Abrasive Waterjet for Machining Advanced Materials. *J. Manuf. Mater. Process.* **2017**, *1*, 11. [CrossRef]
3. Hashish, M. Visualization of the Abrasive-Waterjet Cutting Process. *Exp. Mech.* **1988**, *28*, 159–169. [CrossRef]
4. Cano-Salinas, L.; Sourd, X.; Moussaoui, K.; Le Roux, S.; Salem, M.; Hor, A.; Zitoune, R. Effect of Process Parameters of Plain Water Jet on the Cleaning Quality, Surface and Material Integrity of Inconel 718 Milled by Abrasive Water Jet. *Tribol. Int.* **2023**, *178*, 108094. [CrossRef]
5. Zhang, S. A Review on Abrasive Waterjet and Wire Electrical Discharge Machining—High Speed. *Open Mech. Eng. J.* **2011**, *5*, 178–185. [CrossRef]
6. Hlavacova, I.M.; Geryk, V. Abrasives for Water-Jet Cutting of High-Strength and Thick Hard Materials. *Int. J. Adv. Manuf. Technol.* **2017**, *90*, 1217–1224. [CrossRef]
7. Natarajan, Y.; Murugesan, P.K.; Mohan, M.; Liyakath Ali Khan, S.A. Abrasive Water Jet Machining Process: A State of Art of Review. *J. Manuf. Process.* **2020**, *49*, 271–322. [CrossRef]
8. Zelenak, M.; Valicek, J.; Klich, J.; Zidkova, P. Comparison of Surface Roughness Quality Created by Abrasive Water Jet and CO_2 Laser Beam Cutting. *Teh. Vjesn.* **2012**, *19*, 481–485.
9. Llanto, J.M.; Tolouei-Rad, M.; Vafadar, A.; Aamir, M. Recent Progress Trend on Abrasive Waterjet Cutting of Metallic Materials: A Review. *Appl. Sci.* **2021**, *11*, 3344. [CrossRef]
10. Alberdi, A.; Rivero, A.; López de Lacalle, L.N. Experimental Study of the Slot Overlapping and Tool Path Variation Effect in Abrasive Waterjet Milling. *J. Manuf. Sci. Eng.* **2011**, *133*, 034502. [CrossRef]
11. Gadelmawla, E.S.; Koura, M.M.; Maksoud, T.M.A.; Elewa, I.M.; Soliman, H.H. Roughness Parameters. *J. Mater. Process. Technol.* **2002**, *123*, 133–145. [CrossRef]
12. Khan, A.M.; Gupta, K. Machinability Studies on Abrasive Water Jet Machining of Low Alloy Steel for Different Thickness. *IOP Conf. Ser. Mater. Sci. Eng.* **2020**, *709*, 044099. [CrossRef]
13. Malm, F. Abrasive Waterjet Process Parameters Optimization. Master's Thesis, Western Carolina University, Cullowhee, NC, USA, 2024.
14. Magsipoc, E.; Zhao, Q.; Grasselli, G. 2D and 3D Roughness Characterization. *Rock Mech. Rock Eng.* **2020**, *53*, 1495–1519. [CrossRef]
15. Coba Salcedo, M.F.; Acevedo Peñaloza, C.H.; Valencia, G. Experimental Study of the Correlation the Surface Roughness 2D and 3D in the Honing Process of the Steel Cylinder. *Indian J. Sci. Technol.* **2018**, *11*, 1–9. [CrossRef]
16. Sztankovics, I. Analysis of Selected Function-Defining 2D Surface Roughness Parameters in Tangential Turning. *Cut. Tools Technol. Syst.* **2023**, *98*, 109–115. [CrossRef]
17. Mgherony, A.; Mikó, B.; Farkas, G. Comparison of Surface Roughness When Turning and Milling. *Period. Polytech. Mech. Eng.* **2021**, *65*, 337–344. [CrossRef]
18. Grešová, Z.; Ižol, P.; Vrabeľ, M.; Kaščák, Ľ.; Brindza, J.; Demko, M. Influence of Ball-End Milling Strategy on the Accuracy and Roughness of Free Form Surfaces. *Appl. Sci.* **2022**, *12*, 4421. [CrossRef]
19. Varga, G. Examination of Surface Roughness of Holes of Plastic Parts Drilled under Cryogenic Cooling Conditions. *IOP Conf. Ser. Mater. Sci. Eng.* **2018**, *448*, 012065. [CrossRef]
20. Arencibia, R.V.; Arantes, L.J.; Franco, V.L.D.S.; da Silva, J.A.; Piratelli-Filho, A.; da Silva, L.R.R.; Franco, S.D. Characterization of Turned Surfaces Using 3D Roughness Parameters. *J. Braz. Soc. Mech. Sci. Eng.* **2024**, *46*, 487. [CrossRef]
21. Nagy, A. Influence of Measurement Settings on Areal Roughness with Confocal Chromatic Sensor on Face-Milled Surface. *Cut. Tools Technol. Syst.* **2020**, *93*, 65–75. [CrossRef]

22. Deleanu, L.; Georgescu, C.; Suciu, C. A Comparison between 2D and 3D Surface Parameters for Evaluating the Quality of Surfaces. *Ann. "Dunarea Jos" Univ. Galati Fascicle V Technol. Mach. Build.* **2012**, *30*, 5–12.
23. García Jurado, D.; Garófano, J.E.; Contreras, J.P.; Marcos, M. Proposal of a Correlation Function between 2D and 3D Roughness Parameters. *AIP Conf. Proc.* **2009**, *1181*, 418–426. [CrossRef]
24. Bulaha, N. Calculations of Surface Roughness 3D Parameters for Surfaces with Irregular Roughness. *Eng. Rural. Dev.* **2018**, *23*, 1437–1444.
25. Pawlus, P.; Reizer, R.; Krolczyk, G.M. Modelling and Prediction of Surface Textures after Abrasive Machining Processes: A Review. *Measurement* **2023**, *220*, 113337. [CrossRef]
26. Deltombe, R.; Kubiak, K.J.; Bigerelle, M. How to Select the Most Relevant 3D Roughness Parameters of a Surface. *Scanning* **2014**, *36*, 150–160. [CrossRef]
27. Rosentritt, M.; Schneider-Feyrer, S.; Kurzendorfer, L. Comparison of Surface Roughness Parameters Ra/Sa and Rz/Sz with Different Measuring Devices. *J. Mech. Behav. Biomed. Mater.* **2024**, *150*, 106349. [CrossRef]
28. De Lacalle, L.N.L.; Lamikiz, A.; Salgado, M.A.; Herranz, S.; Rivero, A. Process Planning for Reliable High-Speed Machining of Moulds. *Int. J. Prod. Res.* **2002**, *40*, 2789–2809. [CrossRef]
29. Deleanu, L.; Cantaragiu, A.; Georgescu, C.; Botan, M. Influence of Measurements on 3D Roughness Parameters. *Mech. Test. Diagn.* **2011**, *1*, 42–53.
30. Tchoundjeu, S.; Bigerelle, M.; Robbe-Valloire, F.; Da Silva Botelho, T.; Jarnias, F. How to Select 2D and 3D Roughness Parameters at Their Relevant Scales by the Analysis of Covariance. *Materials* **2020**, *13*, 1526. [CrossRef]
31. Hashish, M. Characteristics of Surfaces Machined With Abrasive-Waterjets. *J. Eng. Mater. Technol.* **1991**, *113*, 354–362. [CrossRef]
32. Alberdi, A.; Rivero, A.; López de Lacalle, L.N.; Etxeberria, I.; Suárez, A. Effect of Process Parameter on the Kerf Geometry in Abrasive Water Jet Milling. *Int. J. Adv. Manuf. Technol.* **2010**, *51*, 467–480. [CrossRef]
33. Harničárová, M.; Valíček, J.; Kušnerová, M.; Kopal, I.; Lupták, M.; Mikuš, R.; Pavelek, Z.; Fabián, M.; Šepelák, V. Structural and Mechanical Changes of AlMgSi0.5 Alloy during Extrusion by ECAP Method. *Materials* **2022**, *15*, 2020. [CrossRef] [PubMed]
34. Guba, N.; Schumski, L.; Paulsen, T.; Karpuschewski, B. Vibration-Assisted Deep Hole Drilling of the Aluminum Material AlMgSi0.5. *CIRP J. Manuf. Sci. Technol.* **2022**, *36*, 57–66. [CrossRef]
35. Maros, Z. Effect of Load Energy on the Form of the Gap at Waterjet Cutting. *Key Eng. Mater.* **2013**, *581*, 304–309. [CrossRef]
36. Maros, Z. Surface Roughness of Aluminium Alloy Cut by Abrasive Waterjet. *Rezan. Instrum. V Tehnol. Sist. Tool Technol. Syst.* **2011**, *80*, 176–180.

Disclaimer/Publisher's Note: The statements, opinions and data contained in all publications are solely those of the individual author(s) and contributor(s) and not of MDPI and/or the editor(s). MDPI and/or the editor(s) disclaim responsibility for any injury to people or property resulting from any ideas, methods, instructions or products referred to in the content.